

Self-consistent model of a positive column in a glow discharge under free-flight and collisional regimes of charged-particle motion

V. S. Egorov,¹ Yu. B. Golubovski,¹ E. Kindel,² I. B. Mekhov,¹ and C. Schimke²

¹*Institut of Physics, St. Petersburg University, Ulianovskaia 1, 198904 Petrodvorets, St. Petersburg, Russia*

²*Institut für Niedertemperatur-Plasmaphysik, Friedrich-Ludwig-Jahn-Strasse 19, 17489 Greifswald, Germany*

(Received 19 March 1999)

We consider the nonlocal theory of a positive column in a glow discharge in two cases, where the mean free path of charged particles is either greater than the discharge tube radius (the free-flight regime) or much less than the radius (the collisional regime). The great bulk of electrons, which determines the density and the discharge current in the axial direction, appears to be trapped by the radial field of a positive column. The electron flux to the wall, which compensates for the ionization in a volume, is determined by fast electrons with energies of the order of wall potential, which are able to leave in a loss cone. The electron kinetic equation, which is solved by averaging it over the radial transits for the two regimes considered, permits us to obtain the electron density and the ionization rate. Thus, we develop the theory of a positive column for the non-Boltzmann electron distribution in the radial field. Under the free-flight regime, this theory is developed by analogy with the Langmuir-Tonks one. Under the collisional regime, the spatial distribution of the potential is obtained from the ion motion equation with the ambipolar diffusion coefficient, which depends on the radial coordinate. The concrete calculations are carried out for the xenon discharge under the free-flight and collisional regimes. The theoretical calculations are compared with the results of experiments on the measurements of the electric field and the densities of metastable and resonance xenon atoms. [S1063-651X(99)13310-5]

PACS number(s): 52.25.Dg, 52.80.Hc, 52.70.Kz, 52.25.Ya

I. INTRODUCTION

The principles of the kinetic theory of a positive column in an inert gas discharge at low pressures and small currents were considered in [1,2]. In these papers, the problem of a joint solution to the electron kinetic equation and the ion motion equation was formulated and ways of solving it were outlined. In [3,4], the concrete calculations were carried out for a set of inert gases in the case of the collisional regime of charged particle motion. The collisional regime takes place when the mean free path of electrons λ_e and that of ions λ_i are much smaller than the discharge tube radius R . So, the application range of the collisional kinetic model is restricted at low pressures by the condition $\lambda_e, \lambda_i < R$. The purpose of this study is to develop the kinetic model of a positive column in an inert gas discharge under the free-flight regime of charged particle motion when the opposite condition $\lambda_e, \lambda_i > R$ is fulfilled. For the first time, such a problem was considered in the work of Langmuir and Tonks [5] under the assumption that in the decelerating radial field, the electron density has Boltzmann distribution. In the present paper, the electron density and the radial potential are determined in a self-consistent way proceeding from a kinetic analysis of electron motion. The comparison between free-flight and collisional models is carried out in the case of a positive column in a xenon discharge. The calculation results are compared with experimental data.

II. KINETIC MODEL OF A POSITIVE COLUMN UNDER FREE-FLIGHT AND COLLISIONAL REGIMES

The peculiarities of electron motion in the potential field of a positive column are related to their acceleration in the longitudinal field E_z and their deceleration in the radial field

E_r , by which, a considerable portion of electrons appears to be trapped by the radial potential $\varphi(r)$. At low pressures, under the free-flight regime, electron motion in the radial direction occurs when the total energy is conserved. Under the collisional regime, when the energy losses in elastic interactions are negligibly small and when the electron energy relaxation length $\lambda_e \sim \sqrt{M/m} \lambda_e$ exceeds the radius R , one can assume that the total energy is also conserved.

Under the collisional regime, the electron momentum relaxation length λ_e is much less than R . That leads to the isotropization of the electron distribution function, and the traditional expansion in Legendre polynomials is obvious. Under the free-flight regime, as was shown in [1], one can also consider the isotropic component of the distribution function $f_0(\varepsilon)$ (with respect to the trapped particles under the condition that the energy gained from the applied electric field between two collisions, $eE_z \lambda_e$, is less than the excitation threshold of atoms ε_1 , i.e., $eE_z \lambda_e / \varepsilon_1 < 1$) and can formulate the kinetic equation, which is the same as the one used for the collisional regime except for the spatially averaged coefficients of the equation.

The kinetic equation for the isotropic component of the distribution function $f_0(\varepsilon)$ is given by [1]

$$\frac{d}{d\varepsilon} \bar{D}_\varepsilon(\varepsilon) \frac{df_0}{d\varepsilon}(\varepsilon) = \overline{v\nu^*}(\varepsilon) f_0(\varepsilon) - \overline{v\nu^*}(\varepsilon + \varepsilon_1) f_0(\varepsilon + \varepsilon_1), \quad (1)$$

where for the free-flight regime coefficient $\bar{D}_\varepsilon(\varepsilon)$ takes the form

$$\bar{D}_\varepsilon(\varepsilon) = \frac{4\sqrt{2}(eE_z)^2}{3m^{3/2}R^2} h(\varepsilon) \int_0^{r_1(\varepsilon)} [\varepsilon - e\varphi(r)]^{3/2} r dr, \quad (2)$$

$$h(\varepsilon) = \frac{\int_0^{r_1(\varepsilon)} [\varepsilon - e\varphi(r)]^{3/2} r dr}{n_a \sqrt{\frac{2}{m}} \int_0^{r_1(\varepsilon)} \sigma_{tr}(\varepsilon - e\varphi(r)) [\varepsilon - e\varphi(r)]^2 r dr}, \quad (3)$$

and for the collisional regime

$$\bar{D}_\varepsilon(\varepsilon) = \frac{4(eE_z)^2}{3mn_a R^2} \int_0^{r_1(\varepsilon)} \frac{[\varepsilon - e\varphi(r)]^{3/2}}{\sigma_{tr}(\varepsilon - e\varphi(r))} r dr. \quad (2')$$

The coefficient on the right-hand side of (1) $\overline{\nu\nu^*}(\varepsilon)$ for the free-flight and collisional regimes is

$$\overline{\nu\nu^*}(\varepsilon) = \frac{4n_a}{mR^2} \int_0^{r_2(\varepsilon)} \sigma^*(\varepsilon - e\varphi(r)) [\varepsilon - e\varphi(r)] r dr. \quad (4)$$

Here, m is the electron mass, n_a is the density of neutral atoms of the inert gas (which is supposed to be uniform), $\sigma_{tr}(w)$ is the elastic transport cross section, $\sigma^*(w)$ is the total inelastic cross section (w is the kinetic energy of the electron), ε_1 is the excitation threshold of atoms, $\varepsilon = w + e\varphi(r)$ is the total energy of the electron, and R is the discharge tube radius. Expressions (2), (2'), (3) contain the quantities averaged over the tube cross section, which is accessible for the particle with energy ε . The function $r_1(\varepsilon)$ is the turning point; it can be defined as $e\varphi(r_1(\varepsilon)) = \varepsilon$. The function $r_2(\varepsilon)$ is the turning point of the electron, which loses energy ε_1 in inelastic collisions, thus $e\varphi(r_2(\varepsilon)) = \varepsilon - \varepsilon_1$.

Under the free-flight regime, the small longitudinal anisotropic component $f_a(\varepsilon, v_z)$ is given by

$$f_a(\varepsilon, v_z) = -eE_z v_z h(\varepsilon) \frac{df_0(\varepsilon)}{d\varepsilon}, \quad (5)$$

where v_z is the longitudinal component of the electron velocity. Under the collisional regime, that anisotropic component is given by

$$f_a(\varepsilon, v_z, r) = f_{1z}(\varepsilon, r) \frac{v_z}{v} = - \frac{eE_z v_z}{n_a \sqrt{\frac{2w}{m}} \sigma_{tr}(w)} \frac{df_0(\varepsilon)}{d\varepsilon}. \quad (5')$$

Under the assumption that the total energy is constant for the radial flights of trapped electrons, the radial anisotropic component of the distribution function is equal to zero.

The kinetic equation (1) should be supplemented by the boundary condition according to the possibility of electron losses on the wall if the electron energy exceeds the wall potential ε_w . The correct solution to the problem includes consideration of the loss cone to the wall. When locating itself in this cone due to collisions, the electron can leave to the wall, which is equivalent to the finite electron loss frequency. In this case, it is necessary to add to the right-hand side of Eq. (1) the additional term averaged over radial electron transits $\overline{\nu\nu_w}(\varepsilon)f_0(\varepsilon)$, where ν_w is the frequency of the

electron losses on the wall [$\overline{\nu\nu_w}(\varepsilon) = 0$ if $\varepsilon < \varepsilon_w$]. The boundary condition for Eq. (1) is the condition of function $f_0(\varepsilon)$ reduction to zero at infinity, i.e.,

$$f_0(\varepsilon)|_{\varepsilon=\infty} = 0. \quad (6a)$$

If one assumes that the frequency of electron losses on the wall is rather great, instead of (6a) one can set the zero boundary condition for the distribution function at the wall potential ε_w to be

$$f_0(\varepsilon)|_{\varepsilon=\varepsilon_w} = 0. \quad (6b)$$

The latter condition corresponds to the so-called ‘‘black-wall’’ approximation.

The normalization condition for the distribution function $f_0(\varepsilon)$ can be written as follows:

$$n_e(\varphi(r)) = \frac{4\pi\sqrt{2}}{m^{3/2}} n_0 \int_{e\varphi(r)}^{\varepsilon_{w,\infty}} f_0(\varepsilon) \sqrt{\varepsilon - e\varphi(r)} d\varepsilon, \quad (7)$$

where n_0 is the electron density at the discharge axis. The symbol $\varepsilon_{w,\infty}$ in the upper limit of the integral takes the value of either ε_w in the black-wall approximation (6b) or infinity if the problem is solved with the loss cone consideration (6a). Expression (7) determines the distribution of the electron density in the decelerating radial field for the nonequilibrium distribution function. In the case of the Maxwell distribution function, this expression gives the Boltzmann dependency $n_e(r) = n_0 e^{-e\varphi(r)/kT_e}$. Knowing the external discharge parameter, current i , one can determine the value of n_0 . The current density $j_z(r)$ with the anisotropic component of the distribution function (5) and (5') takes the forms

$$j_z(r) = \frac{8\pi\sqrt{2}}{3m^{5/2}} e^2 E_z n_0 \int_{e\varphi(r)}^{\varepsilon_{w,\infty}} [\varepsilon - e\varphi(r)]^{3/2} h(\varepsilon) \left| \frac{df_0}{d\varepsilon}(\varepsilon) \right| d\varepsilon, \quad (8)$$

$$j_z(r) = \frac{8\pi}{3m^2 n_a} e^2 E_z n_0 \int_{e\varphi(r)}^{\varepsilon_{w,\infty}} \frac{[\varepsilon - e\varphi(r)]}{\sigma_{tr}(\varepsilon - e\varphi(r))} \left| \frac{df_0}{d\varepsilon}(\varepsilon) \right| d\varepsilon, \quad (8')$$

respectively, for the free-flight and collisional regimes. By integrating Eqs. (8) and (8') over the radius, and by changing the order of integration, one comes to the following expression for the discharge current i :

$$i = \frac{4\pi^2}{mE_z} R^2 n_0 \int_0^{\varepsilon_{w,\infty}} \left| \frac{df_0}{d\varepsilon}(\varepsilon) \right| \bar{D}_\varepsilon(\varepsilon) d\varepsilon,$$

where the coefficient $\bar{D}_\varepsilon(\varepsilon)$ is defined by expressions (2) and (2') for the two considered electron kinetic regimes.

By using the distribution function, one can obtain the rates of direct $I_d(r)$ and stepwise $I_s(r)$ ionizations

$$I_d(r) = \frac{8\pi}{m^2} n_0 n_a \int_{\varepsilon_d + e\varphi(r)}^{\varepsilon_{w,\infty}} \sigma_d(\varepsilon - e\varphi(r)) \times f_0(\varepsilon) [\varepsilon - e\varphi(r)] d\varepsilon, \quad (9)$$

$$I_s(r) = \sum_k n_k(r) \nu_{ki}(r),$$

$$\nu_{ki}(r) = \frac{8\pi}{m^2} n_0 \int_{\varepsilon_k + e\varphi(r)}^{\varepsilon_{w,\infty}} \sigma_k(\varepsilon - e\varphi(r)) f_0(\varepsilon) [\varepsilon - e\varphi(r)] d\varepsilon, \quad (10)$$

where $\sigma_d(w)$ and $\sigma_k(w)$ are the cross sections of direct and stepwise ionizations, $n_k(r)$ are the densities of excited atoms, which are involved in the processes of stepwise ionization, and ε_d and ε_k are the threshold values of these processes.

To obtain the stepwise ionization rate, the balance equations for low excited metastable and resonance states must have been solved. In the equations for resonance levels, it is necessary to take into account the effect of radiation reabsorption on the basis of the integral Biberman-Holstein equation [6,7] applied to cylindrical geometry. The balance equations in the two-level approximation are

$$W_m(r) + n_r(r) n_e(r) k_{rm} = n_m(r) [\nu_{mi}(r) + n_e(r) k_{mp} + n_e(r) k_{mr} + \nu_d],$$

$$W_r(r) + n_m(r) n_e(r) k_{mr} + A \int_0^R n_r(r') K(r, r') r' dr' = n_r(r) [A + \nu_{ri}(r) + n_e(r) k_{rp} + n_e(r) k_{rm} + \nu_d], \quad (11)$$

$$K(r, r') = \frac{1}{4\pi} \int_0^{2\pi} d\theta \int_{-\infty}^{\infty} \frac{dz}{z^2 + q^2} \int_0^{\infty} \varepsilon_\nu k_\nu e^{-k_\nu \sqrt{z^2 + q^2}} d\nu,$$

$$q^2 = r^2 + r'^2 - 2rr' \cos \theta,$$

where $\nu_{mi}(r)$ and $\nu_{ri}(r)$ are the frequencies of level deactivation due to stepwise ionization (10), k_{mr} and k_{rm} are the rate constants of the resonance and metastable level mixing, k_{mp} and k_{rp} are the rate constants of the level deactivation due to stepwise excitation of the high-lying states, ν_d is the frequency of the atom transits to the wall, and A is the probability of spontaneous radiation. The level excitation rate $W_{m,r}(r)$ can be obtained in terms of the distribution function

$$W_{m,r}(r) = \frac{8\pi}{m^2} n_a n_0 \int_{\varepsilon_{m,r} + e\varphi(r)}^{\varepsilon_{w,\infty}} \sigma_{m,r}^*(\varepsilon - e\varphi(r)) \times f_0(\varepsilon) [\varepsilon - e\varphi(r)] d\varepsilon, \quad (12)$$

where $\sigma_m^*(w)$ and $\sigma_r^*(w)$ are the cross sections of the corresponding level excitation and ε_m and ε_r are the thresholds of these processes. The integral operator in Eq. (14) describes the absorption of photons at the points with radial coordinate r (hence the appearance of the resonance atoms at these points), which have been emitted at points r' , z , θ , integrated over the whole tube volume. Here, ε_ν and k_ν are the emission and absorption line contours. The second equation in (11) can be solved, for example, by using the reduction to the set of linear algebraic equations as has been described in [8,9].

Thus, the analysis of the electron kinetics permits us to derive the electron density and the total ionization rate, which are necessary for solving the self-consistent problem of the mutual formation of the distribution function and the potential field.

III. SOLUTION TO THE SELF-CONSISTENT PROBLEM OF THE MUTUAL FORMATION OF THE DISTRIBUTION FUNCTION AND THE POTENTIAL FIELD

In the case of the free-flight regime, the problem under analysis can be solved by analogy with the Langmuir-Tonks theory [5] for plasma and layer. The electron density, which is obtained using the nonequilibrium distribution function, is defined by formula (7). One can obtain the ion density $n_i(r)$ from the condition that all ions which appear at the points $r' < r$ due to ionization leave through the cylinder surface at radial coordinate r , when being accelerated by the radial field under the free-flight regime

$$n_i(r) = \frac{1}{r} \int_0^r \frac{I(r') r' dr'}{\sqrt{\frac{2}{M} [e\varphi(r) - e\varphi(r')]}} \quad (13)$$

where M is the ion mass and $I(r)$ is the total ionization rate,

$$I(r) = I_d(r) + I_s(r). \quad (14)$$

In the discharge plasma region, the condition of quasineutrality $n_e \approx n_i$ is fulfilled. By applying the Abel transformation to Eq. (13) [2], one deduces integral differential equation for the function $r(\varphi)$ in the following form:

$$r \frac{dr}{d\varphi} = \frac{1}{\pi} \sqrt{\frac{2e}{M}} \frac{1}{I(\varphi)} \frac{d}{d\varphi} \int_0^\varphi \frac{n_i(\varphi') r(\varphi') d\varphi'}{\sqrt{\varphi - \varphi'}}. \quad (15)$$

Expressions (9), (10), (14) define the ionization rate, and expression (7) defines the ion density for the quasineutral plasma, which is equal to the electron one. By analogy with Langmuir-Tonks theory, the solution of the equation for plasma (15) $r(\varphi)$ has a maximum at the point φ_0 , and $d\varphi/dr \rightarrow \infty$ at this point, which corresponds to the bound of the quasineutral region. If the Debye radius is less than the tube radius, one can assume that this point corresponds to the radius R ,

$$r(\varphi_0) = R. \quad (16)$$

The quantity φ_0 determines the potential fall in the quasineutral plasma. The near-wall drop of potential Δ is equal to the difference between the wall potential ε_w and the potential $e\varphi_0$,

$$\Delta = \varepsilon_w - e\varphi_0. \quad (17)$$

The detailed description of the solution to the problem under the collisional regime was presented in [3,4]. The ion motion equation takes the form

$$\frac{1}{r} \frac{d}{dr} r b_i n_i(r) \frac{d\varphi(r)}{dr} = I(r), \quad (15')$$

where b_i is the ion mobility. This equation can be reduced to the ambipolar diffusion equation with the coefficient, which depends on the radial coordinate [3]. The expression

$$e\varphi(R) = \varepsilon_w \quad (16')$$

is the analogue of the condition (16). Furthermore, by twice integrating Eq. (15') one derives the balance equation

$$\frac{b_i}{e} \int_0^{\varepsilon_w} n_e(e\varphi) de\varphi = \int_0^R \frac{dr}{r} \int_0^r I(r') r' dr'. \quad (18)$$

The equality between the ionizations and the electron transits to the wall is necessary in order to provide the steady-state discharge. In the framework of the model considered, the electron flux to the wall can be obtained from Eq. (1) as the flux in the energy space at the energy ε_w . Under both the free-flight and the collisional regimes, for the number of electron transits to the wall per unit discharge length and unit time, that approach gives

$$2\pi R j_w = \frac{4\pi^2}{m^2} R^2 n_0 \bar{D}_\varepsilon(\varepsilon_w) \left| \frac{df_0}{d\varepsilon}(\varepsilon_w) \right|$$

in the black-wall approximation, and

$$2\pi R j_w = \frac{4\pi^2}{m^2} R^2 n_0 \left[\bar{D}_\varepsilon(\varepsilon_w) \left| \frac{df_0}{d\varepsilon}(\varepsilon_w) \right| - \int_{\varepsilon_w}^{\varepsilon_w + \varepsilon_1} \frac{1}{v\nu^*(\varepsilon)} f_0(\varepsilon) d\varepsilon \right]$$

when considering the loss cone.

The charged particle balance equation can be written in the form

$$2\pi R j_w = 2\pi \int_0^R I(r) r dr. \quad (19)$$

The algorithm of the solution to the self-consistent problem can be represented in the following way. One takes the approximation of the trial potential using three parameters in the form

$$e\varphi(z, r) = -eE_z z + e\varphi(r),$$

$$e\varphi(r) = \begin{cases} \beta\varepsilon_1 \left(\frac{r}{R}\right)^2 & \text{if } r < R, \\ \varepsilon_w & \text{if } r = R. \end{cases} \quad (20)$$

The parameter $\beta\varepsilon_1$ corresponds to the fall of the trial potential in the quasineutral plasma. Then, one can average the coefficients of the kinetic equation over the potential (20) according to expressions (2)–(4). The kinetic equation (1) with the boundary condition (6a) or (6b) depending on the approximation is numerically solved. By using the calculated distribution function, which depends on the three parameters E_z , ε_w , β , the electron density $n_e(r)$, Eq. (7), and the ionization rate $I(r)$ [Eqs. (9), (10), (14)] are then deduced, and the equation for the potential (15) or (15') is solved. Varying the parameters of the trial potential, it is necessary to

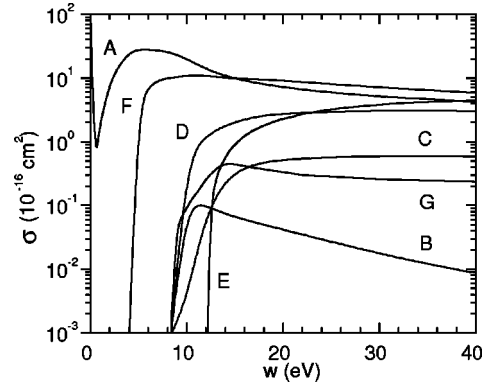


FIG. 1. The cross sections of electron-atom collisions in xenon used in the solution to the kinetic equation and calculation of excitation and ionization rates: A, elastic transport cross section; B, metastable level 3P_2 excitation; C, resonance level 3P_1 excitation; D, total excitation cross section; E, direct ionization; F, stepwise ionization; G, effective cross section of metastable level 3P_2 excitation (cascade excitations are taken into account); A–F: [10], G: [11].

fulfill the conditions (16),(19) and the equality $\beta\varepsilon_1 = e\varphi_0$ for the free-flight regime, and to satisfy the conditions (16'), (19), and (18) for the collisional regime. The solution of (15) or (15') gives the required distribution of potential $\varphi(r)$ for the parameters E_z , ε_w , and β , which were determined in that way.

IV. RESULTS AND DISCUSSIONS

Concrete calculations were carried out for a xenon discharge at a current of 100 mA, in the range of pressures $0.01 < p < 0.15$ Torr; the discharge tube radius was equal to 0.32 cm. The cross sections of elementary processes presented in Fig. 1 were used. To obtain the distribution function, these cross sections were averaged over the trial potential (20) according to expressions (2)–(4); the kinetic equation (1) was numerically solved with the boundary condition (6a) or (6b). The numerical method of solving Eq. (1) is based on its conversion into a set of linear algebraic equations.

The results of the distribution function calculation, which was carried out in the framework of the solution to the self-consistent problem under the free-flight kinetics with both the zero boundary condition and the loss cone taken into account, are presented in Fig. 2. The coefficient $\overline{v\nu_w}(\varepsilon)$ was defined as

$$\overline{v\nu_w}(\varepsilon) = \begin{cases} 0 & \text{if } \varepsilon < \varepsilon_w; \\ 2\pi\nu_0 \sqrt{\frac{2(\varepsilon - \varepsilon_w)}{m}} & \text{if } \varepsilon \geq \varepsilon_w, \end{cases}$$

where ν_0 is some mean value of the electron-atomic elastic collision frequency. The consideration of the loss cone leads to a decrease in the value of the wall potential ε_w ; nevertheless, in the energy range of excitations and ionizations, the difference between the distribution functions calculated in two approximations is not significant. That being the case, the simpler approximation was used to develop the self-consistent model.

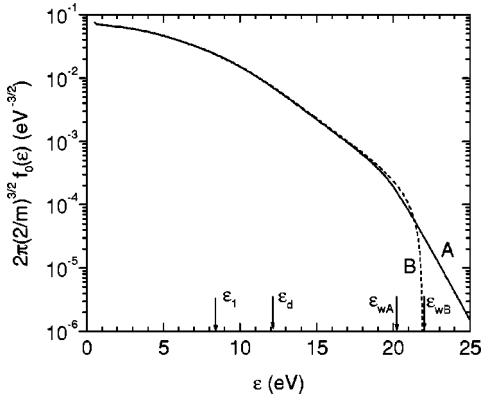


FIG. 2. Comparison between the kinetic equation solution for the free-flight regime of electron kinetics with the loss cone taken into account (solid curve A) and that under the black-wall approximation (dashed curve B) obtained in the framework of the solution to the self-consistent problem; ε_1 is the first excitation threshold, ε_d is the ionization threshold, and ε_{wA} and ε_{wB} are the wall potentials obtained by using the distribution functions A and B, respectively; Xe, $p=0.04$ Torr, $i=100$ mA, $R=0.32$ cm, $E_z=3.32$ V/cm.

The kinetic equation (1) for the isotropic component of the distribution function has a different form for the free-flight and collisional regimes. This difference is related to the forms of the coefficient $\bar{D}_\varepsilon(\varepsilon)$, Eqs. (2) and (2'). In Fig. 3, the distribution functions obtained in the framework of the free-flight and collisional models in the same potential field $e\varphi(z, r)$ and with the same boundary conditions are compared.

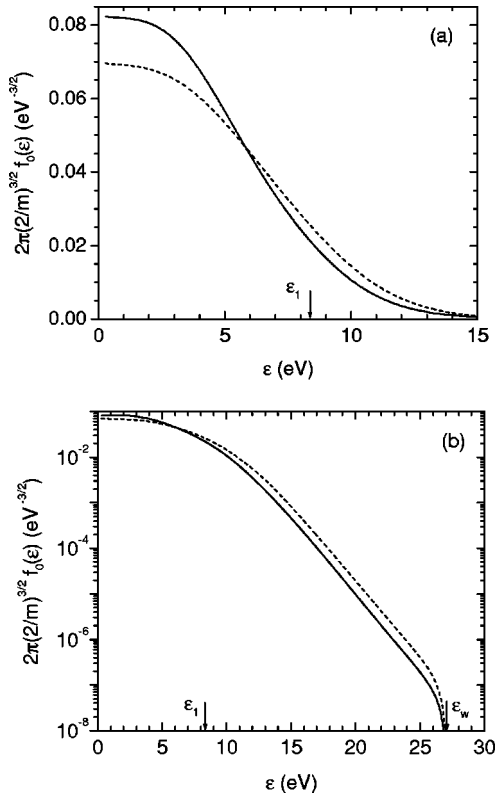


FIG. 3. Comparison of solutions to the kinetic equation for the free-flight regime (solid curve) and that for the collisional regime (dashed curve); (a) linear scale, (b) logarithmic scale; Xe, $p=0.10$ Torr, $i=100$ mA, $R=0.32$ cm, $E_z=3.50$ V/cm.

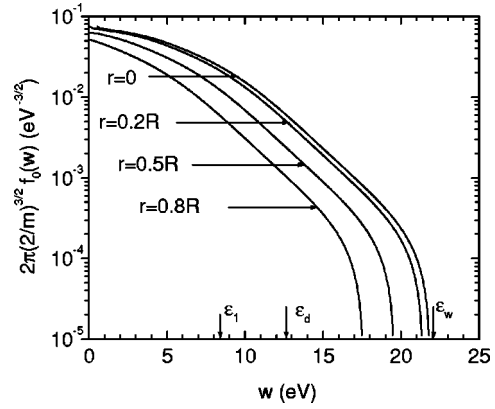


FIG. 4. Kinetic energy distribution function at different radial points obtained in the framework of the solution to the self-consistent problem for the free-flight regime; Xe, $p=0.04$ Torr, $i=100$ mA, $R=0.32$ cm, $E_z=3.32$ V/cm.

In Fig. 4, the isotropic component of the kinetic energy distribution function at different radial points calculated in the black-wall approximation under the free-flight regime is displayed. The specific feature of a nonlocal formation of the electron distribution function consists of its sufficient deformation over radius, due to a large depletion with fast electrons in the peripheral regions of the discharge tube. This leads to a steeper radial dependency of the ionization and excitation rates than that of the electron density. Moreover, in this case the electron kinetic mean energy depends on the radial coordinate. These facts are shown in Fig. 5.

The calculations of the excitation rates and the populations of the metastable 3P_2 and resonance 3P_1 levels were carried out using Eqs. (11) and (12). Considering the balance equations for the populations of these levels, the processes of direct excitation from the ground state, mixing due to collisions with electrons, stepwise excitation of high-lying states, stepwise ionization, departures to the wall, and resonant radiation outcome were taken into account. According to estimations, the other processes (molecule creation, chemoionization, etc.) are not significant under the conditions considered.

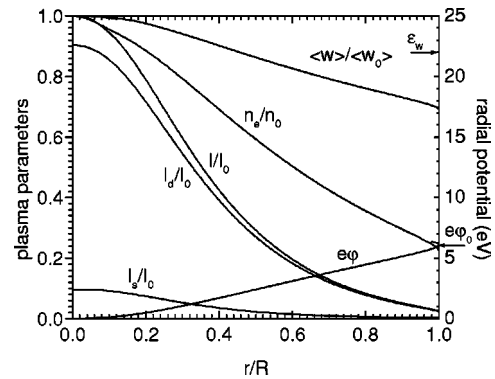


FIG. 5. Relative radial distributions of the potential $e\varphi$ and the macroscopic plasma parameters: mean energy $\langle w \rangle$, electron density n_e , direct I_d , stepwise I_s , and total I ionization rates obtained in the framework of the solution to the self-consistent problem for the free-flight regime. Axial values: $\langle w_0 \rangle = 5.82$ eV, $n_0 = 2.44 \times 10^{11}$ cm $^{-3}$, $I_0 = 3.75 \times 10^{17}$ cm $^{-3}$ s $^{-1}$; Xe, $p=0.04$ Torr, $i=100$ mA, $R=0.32$ cm, $E_z=3.32$ V/cm.

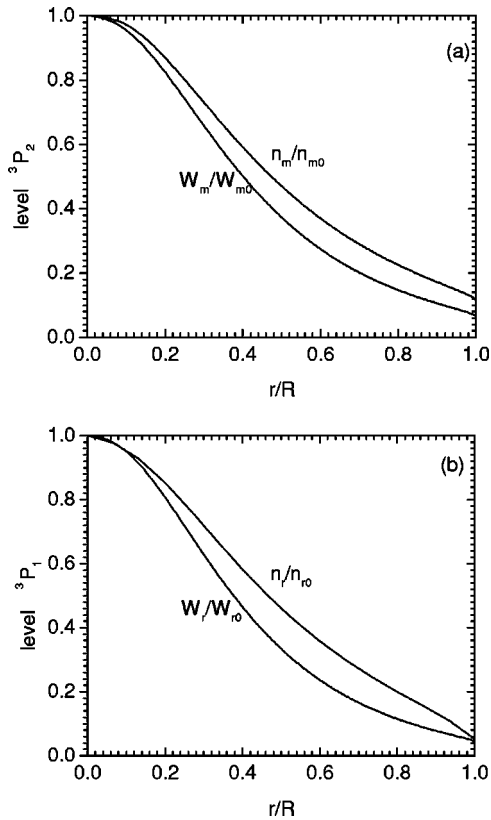


FIG. 6. Relative radial distributions of excitation rates $W_{m,r}$ and populations $n_{m,r}$ of (a) metastable state 3P_2 , (b) resonance state 3P_1 obtained in the framework of the solution to the self-consistent problem for the free-flight regime. Axial values: $W_{m0} = 2.73 \times 10^{17} \text{ cm}^{-3} \text{ s}^{-1}$, $n_{m0} = 1.74 \times 10^{12} \text{ cm}^{-3}$, $W_{r0} = 1.47 \times 10^{17} \text{ cm}^{-3} \text{ s}^{-1}$, $n_{r0} = 2.69 \times 10^{11} \text{ cm}^{-3}$; Xe, $p = 0.04 \text{ Torr}$, $i = 100 \text{ mA}$, $R = 0.32 \text{ cm}$, $E_z = 3.32 \text{ V/cm}$.

In the range of pressure corresponding to the free-flight electron kinetics, the stepwise transits to high-lying levels are negligible. Herewith, in connection with the determination of the metastable atom excitation rate, it is necessary to note the following. As the literature on data analysis shows (for example, [11]), the process of the metastable atom generation is mainly determined by the cascade radiative transits from the configuration $5p^56p$ and the more high-lying electron configurations of the xenon atom. This circumstance was taken into account by using the corresponding cross section of the 3P_2 level excitation presented in [11].

In the range of pressures, corresponding to the collisional electron kinetics, the stepwise transits to the more high-lying levels and the subsequent transits to the continuum are the most significant processes in the deactivations of the 3P_2 and 3P_1 levels. This circumstance was taken into account by bringing the additional flux from the metastable and resonance levels into the expression for the ionization rate $I(r)$ (the approximation of the instant high-lying state ionization).

Solving the integral Biberman-Holstein equation, the contours of radiation and absorption lines were supposed to be dispersive, since in the situation considered the absorption coefficients are sufficiently great and the dispersive wing of the line plays the most important role in the radiation outcome.

In Fig. 6, the radial distributions of the excitation rates

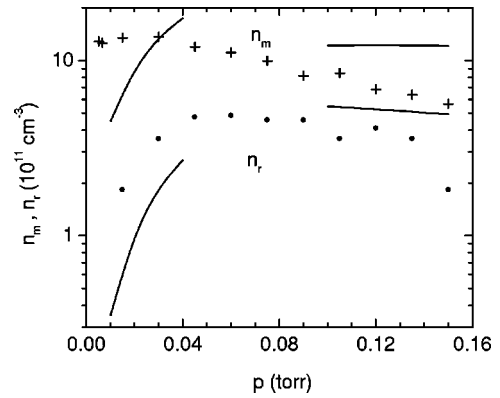


FIG. 7. Comparison between experimental and theoretical dependencies of the metastable state 3P_2 (crosses for experiment) and the resonance state 3P_1 (circles for experiment) populations on the pressure; solid curves denote calculations by the free-flight model in the range of pressures $0.01 < p < 0.04 \text{ Torr}$ and by the collisional one in the range of pressures $0.10 < p < 0.15 \text{ Torr}$; Xe, $i = 100 \text{ mA}$, $R = 0.32 \text{ cm}$.

and excited state populations are compared. These figures show that the radial distributions of the excited particle densities are broader than those of the excitation rates. The latter is related to the main mechanisms of the excited level deactivation. These mechanisms are different for the resonance and metastable levels.

The main channels of metastable level deactivation are the stepwise ionization and the departures to the wall under the free-flight regime. The broadening of the metastable atom density profile in comparison with that of the excitation rate is related to competition between these processes, besides the fact that it is the stepwise ionization that leads to the broadening. For the resonance atoms, the observed broadening of the density profile is related to resonant radiation trapping and the excited atom production due to this effect. The theoretical calculations were compared with the results of experiments on the measurements of the metastable and resonance xenon level populations by the Rozhdestvensky hook method.

The optical scheme of the measurement of the densities of the excited xenon atoms in the 3P_2 and 3P_1 states corresponds to the classical scheme of the hook method modified according to modern experiment potentialities. The dye laser pumped by the pulse discharge nitrogen laser was used as a source of the continuous spectrum. In the optical scheme, instead of the stationary spectral device, a combination of optical elements easy to replace on the vibrostable experimental table (lenses, mirrors, diffraction gratings) was used. Using the 1200 grooves/mm grating, the spectral dispersion of the system reached the value of 0.2 nm/cm . The hook interference picture was registered by video camera and treated by computer. The treatment of the hook picture was based on the so-called vernier method [12]. A detailed description of the experiment and treatment method was presented in [13]. The length of the discharge tube was 60 cm , the radius 0.32 cm . The discharge current was equal to 75 mA , 100 mA , and 125 mA . In addition, measurements of the discharge longitudinal electric field were carried out.

In Figs. 7 and 8, the theoretical dependencies of the metastable 3P_2 and resonance 3P_1 xenon level populations at the

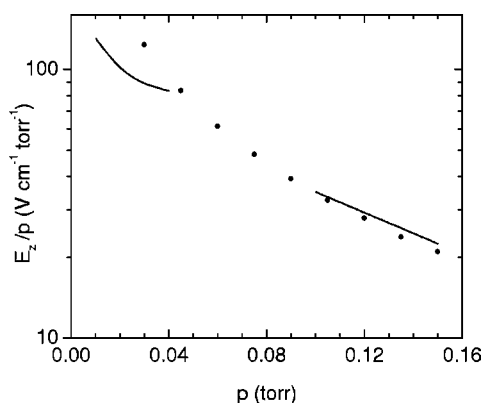


FIG. 8. Comparison between experimental (circles) and theoretical (solid curve) dependencies of the reduced field E_z/p on the pressure; calculations were carried out using the free-flight model in the range of pressures $0.01 < p < 0.04$ Torr and the collisional one in the range of pressures $0.10 < p < 0.15$ Torr; Xe, $i = 100$ mA, $R = 0.32$ cm.

discharge axis and that of the reduced field E_z/p on the pressure are compared with experimental dependencies. In the theoretical calculations, the free-flight model of charged particle motion was applied in the range of pressures $0.01 < p < 0.04$ Torr, whereas the collisional one was applied in the range of $0.10 < p < 0.15$ Torr. The figures show that the proposed theory reaches satisfying agreement with experiment in the absolute values of the metastable and resonance level populations and in the absolute value of the reduced field, in spite of the existing uncertainty in the constants of elementary processes. The theory describes the tendency of the level populations to increase with pressure growth in the range of $0.01 < p < 0.04$ Torr (the free-flight regime) and its tendency toward saturation in the range of $0.10 < p < 0.15$ Torr (the collisional regime). The reduced field decreases

with the growth of pressure observed in experiment also falls within the framework of the proposed theory.

V. CONCLUSION

The solution to the kinetic equation for the isotropic component of the electron distribution function in a positive column of a glow discharge was analyzed under the conditions that the energy relaxation length of electrons is much greater than the discharge tube radius R and that the free path of electrons is either greater than R (the free-flight regime of electron motion) or less than R (the collisional regime). Using the calculated distribution function, the distributions of the electron density that has a non-Boltzmann form and the ionization rates were obtained. These functions were involved in the solution to the ion motion equation in the two limiting cases, where, in the accelerating radial field, the ions move either without collisions (the Langmuir-Tonks theory analogue) or under the diffusion regime (the Schottky theory analogue). The ion equation solution permits one to obtain in a self-consistent way the longitudinal electric field and the radial potential and hence to solve the problem of the mutual formation of the distribution function and the potential field. In the framework of the proposed theory, the main macroscopic plasma parameters — the electron densities, the mean energies, the excitation and ionization rates, the populations of the metastable and resonance levels — and the radial distributions of these parameters were obtained in the case of the xenon discharge at low pressures. Under the same conditions, experiments on the measurements of the longitudinal electric field and the populations of the xenon metastable and resonance levels were carried out on the basis of the Rozhdestvensky hook method. Comparison of the theoretical and experimental data displays satisfying agreement in the absolute values as well as in the relative dependencies of the observed parameters on the pressure.

-
- [1] L. D. Tsendin and Yu. B. Golubovski, *Zh. Tekh. Fiz.* **47**, 1839 (1977) [*Sov. Phys. Tech. Phys.* **22**, 1066 (1977)].
- [2] L. D. Tsendin, *Zh. Tekh. Fiz.* **48**, 1569 (1978) [*Sov. Phys. Tech. Phys.* **23**, 890 (1978)].
- [3] J. Behnke, Yu. B. Golubovski, S. U. Nisimov, and I. A. Porokhova, *Contrib. Plasma Phys.* **36**, 75 (1996).
- [4] Yu. B. Golubovski, I. A. Porokhova, J. Behnke, and J. F. Behnke, *J. Phys. D* **32**, 456 (1999).
- [5] I. Langmuir and L. Tonks, *Phys. Rev.* **34**, 876 (1924).
- [6] L. M. Biberman, *Zh. Eksp. Teor. Fiz.* **17**, 416 (1947).
- [7] T. Holstein, *Phys. Rev.* **72**, 1220 (1947).
- [8] Yu. B. Golubovski, Yu. M. Kagan, and R. I. Lyagushchenko, *Opt. Spektrosk.* **31**, 22 (1971).
- [9] Yu. B. Golubovski and R. I. Lyagushchenko, *Opt. Spektrosk.* **40**, 215 (1976) [*Opt. Spektrosk.* **40**, 124 (1976)].
- [10] J. Meunier, Rh. Belenguer, and J. B. Bouef, *J. Appl. Phys.* **78**, 731 (1995).
- [11] A. A. Mityureva and V. V. Smirnov, *J. Phys. B* **2**, 1869 (1994).
- [12] R. J. Sandeman, *Appl. Opt.* **18**, 3873 (1979).
- [13] E. Kindel and C. Schimke, *Contrib. Plasma Phys.* **36**, 711 (1996).